Electronic States in a Finite Carbon Nanotube: A One-Dimensional Quantum Box

Angel Rubio,[1,*] Daniel Sánchez-Portal,[2] Emilio Artacho,[2] Pablo Ordejón,[3] and José M. Soler[2]
[1]*Departamento de Física Teórica, Universidad de Valladolid, 47011 Valladolid, Spain*
[2]*Departamento de Física de la Materia Condensada and Instituto Nicolás Cabrera, C-III, Universidad Autónoma de Madrid, 28049 Madrid, Spain*
[3]*Departamento de Física, Universidad de Oviedo, 33007 Oviedo, Spain*
(Received 9 November 1998)

The theoretical scanning-tunneling-spectroscopy image catalog of quantized molecular orbitals of finite armchair carbon nanotubes deposited on a gold (111) surface is presented. Just four different three-dimensional standing-wave (SW) patterns are obtained for electrons close to the Fermi level. The experimental observations of a SW modulation of 0.74 nm and peak pairing in line scans are understood in sight of our results. We show that SW patterns can be explained in terms of the simple Hückel model, but the associated energies, relevant to spectroscopic and transport measurements, are very sensitive to different effects beyond that model including the relaxed geometry, the electronic self-consistency in the finite tubes, and the interaction with the substrate. [S0031-9007(99)08999-1]

PACS numbers: 73.50.–h, 61.16.Ch, 61.48.+c, 72.10.–d

Carbon nanotubes are graphitic cylinders of diameters as small as 1 nm and lengths up to several microns [1]. This geometry makes them excellent candidates for use as nanoscopic quantum wires. Band theory predicted [2,3] and experiments confirmed [4] the interplay between geometry and electronic properties and that single-wall "armchair" nanotubes are metallic. A conducting nanotube cut to a finite length should then display the standing waves (SW) characteristic of a one-dimensional (1D) particle-in-a-box model. Evidence of 1D quantum confinement in these tubes has already been obtained [5,6], but the SW states have only recently been observed in 1D scans of scanning tunneling spectroscopy (STS) [7]. The key issue in the experiments comes from the subtle but profound difference between infinite vs finite tube states. While the first are continuous in energy and structureless in space (beyond the underlying atomic periodicity), the second have a complex structure in energy and space. This difference turns scanning tunneling microscopy (STM) into a powerful tool to measure the wave functions and electronic energies of carbon nanotubes. In this Letter we present the energies and three-dimensional shapes of these SW states, based on large-scale first-principles calculations of finite armchair tubes deposited on a gold surface, as in the experiment. Our calculations validate the experimental findings and show that tube curvature, termination, structural relaxation, and substrate interaction *do not* alter significantly the Hückel-STM patterns [8].

The armchair (n, n) single-wall nanotubes can be regarded as the result of rolling one sheet of graphite (graphene) in the direction of one of the bonds [9]. The resulting structure has a periodicity $a = 0.246$ nm along the tube axis, with $4n$ atoms along the perimeter, arranged in two rows that resemble a chain of armchairs (see Fig. 1a). Their metallic character arises from two π bands crossing the Fermi level at wave vector $k_F \approx 2\pi/3a$, wavelength $\lambda_F \approx 3a$, and group velocity $v_F = \pm 8.1 \times 10^5$ m/s. SW patterns can be produced in either metal-semiconductor nanotube junctions [10] or in a finite length L nanotube [11] where quantum confinement along the tube axis reduces the continuous band structure to a discrete set of molecular levels [12]. In the simple 1D particle-in-a-box model, the electron eigenstates are SW of the form $\sin(kx)$, with $k = m\pi/L$ and m integer. In STS scans, which essentially see the square of the wave functions close to the Fermi level, we expect two maxima, repeating with a periodicity $\lambda_F \approx 0.74$ nm. This observation requires an energy resolution better than the SW energy separation $\Delta E = hv_F/2L = (1.68\ \text{eV nm})/L$, and an electron coherence length larger than the tube length [13]. These conditions were matched by the experiments of Ref. [7], performed with tubes of $L \sim 30$ nm at $T = 4$ K.

Although the basic SW observation seems to be explained by the particle-in-a-box model, further insight is required to understand the position of the observed peaks, both in energy and space. To get more insight into the role of those effects we first perform a study using the usual Hückel model for a π-bonded graphite sheet [9] that retains only the nearest-neighbor interaction between p_z orbitals oriented perpendicular to the tube axis [14]. In this model, the wave functions of the band states crossing the Fermi level ($k_F = 2\pi/3a$) are $\psi_i(x) = c_i \sin(kx)$, with $c_1 = c_2 = -c_3 = -c_4$ for the bonding states (descending band), and $c_1 = -c_2 = -c_3 = c_4$ for the antibonding solutions. Here, i labels four consecutive atoms along an armchair, x is the coordinate parallel to the tube axis, and $k = m\pi/L$, where $L = (l + 1)a/2$ is the effective tube length, with l the number of atomic tube layers. When $k = 2\pi/3a$ is one of the allowed values (this occurs for $l = 3r - 1$, with r an integer), the solution at the Fermi level repeats exactly every $\lambda = 3a$. When k is not exactly $2\pi/3a$, either because the tube length does not allow it or because we have to consider states in the

 0031-9007/99/82(17)/3520(4)$15.00

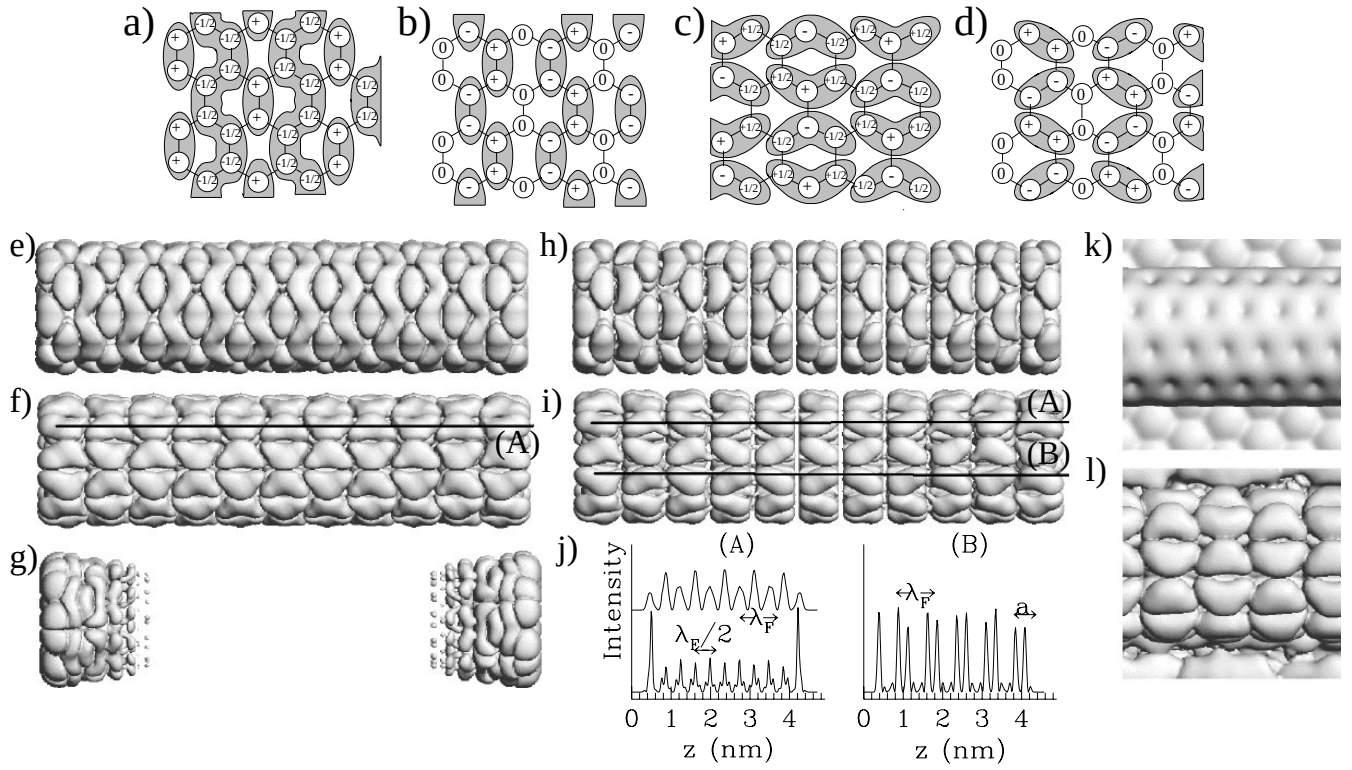

FIG. 1. (a)–(d): Schematic Hückel catalog of the electron wave functions for finite armchair tubes near the Fermi level. (e)–(l): Results from *ab initio* calculations. (e) to (i) show simulated STS images of finite isolated tubes with two different lengths. (e) and (f) show the HOMO and LUMO states of the 4.18 nm tube, respectively. (h) and (i) show the same for the 4.06 nm tube. (g) is a surface state of the longer tube. Solid lines in the images correspond to the line scan shown in panel (j): (A) for equidistant-peak scan corresponding to scan through the middle of the bonds forming an angle with the tube axis, (B) for peak-pairing scan corresponding to scan through the bonds perpendicular to the tube axis. The bottom/top (A) curves in (j) correspond to the marked line scans in panels (f) and (i), respectively. (k) and (l) show *ab initio* results for a $(5,5)$ nanotube deposited on a Au(111) surface. (k) shows the simulated STM image for a positive bias of 0.5 eV showing no SW pattern, because of the integration of several states. (l) shows the HOMO of the system. An infinite tube was calculated on Au, for computational reasons, and the SW pattern was recovered by summing the k and $-k$ Bloch states. In the calculations we used a minimal-basis set of (sp) orbitals for carbon and (spd) for gold, and a cutoff of 50 Ry for the density grid. Lattice parameters for graphene and fcc gold were within 1% of experiment. The finite $(6,6)$ tubes were fully relaxed resulting in dimer formation (with interatomic distances of 0.127 nm) at the tube ends to reduce dangling bonds, while the body of the tube remained essentially unchanged with respect to the infinite tube (bond length of $\sim$0.142 nm). The gold (111) substrate was described with a slab of six layers, which was relaxed with the bottom layer fixed to the bulk positions. The computed work function of the Au(111) surface is 5.0 eV, close to the experimental work function ($\sim$5.3 eV). A relaxed $(5,5)$ nanotube was then deposited on the Au surface, with its axis along the (110) surface direction. The tube-substrate distance was set to the value that minimizes the total energy ($\sim$0.27 nm).

neighborhood of k_F (i.e., k and $k + \Delta k$), we can expand $\sin[(k + \Delta k)x] = \sin(\Delta kx)\cos(kx) + \cos(\Delta kx)\sin(kx)$. For $\Delta k = \pi/L$ and $x \sim L/2$ (near the center of the tube), the second term vanishes, and we may simply substitute $\sin(kx)$ by $\cos(kx)$ in the wave functions, but still with $k = 2\pi/3a$ (the small difference, $k - 2\pi/3a$, only introduces a slowly modulation of the wave function). Figures 1a–1d show the four wave function patterns obtained by combining the bonding and antibonding solutions with the sine and cosine envelopes. They constitute the *complete catalog* of STS patterns to be expected near the Fermi level at the center of an armchair nanotube.

Since experiments give only a few line scans along the tube axis, we test our predictions with the aid of large-scale first-principles calculations. We use the SIESTA program [15], based on density-functional theory, in the local-density approximation [16], using norm-conserving pseudopotentials [17] and a basis set of atomic orbitals [18]. The structures of the tubes are relaxed following the calculated atomic forces. In the simplest approximation [19], the differential conductance dI/dV is proportional to the local density of states (LDOS) of the substrate at the tip center. For a molecule with discrete states, the LDOS is given by the squared wave function amplitudes. Therefore, we simulate STS images as isosurfaces of constant $|\psi_i(\mathbf{r})|^2$ for a given electronic state i. Although tip-convolution effects are neglected, the general shape of STS images remains unchanged [8,20].

Figure 1 shows the highest occupied molecular orbital (HOMO) and the lowest unoccupied molecular orbital (LUMO) for two isolated armchair (6,6) but finite tubes of different lengths. The overall similarity of these images

with those of the Hückel catalog is very remarkable. The length of the first tube does not allow the $k = 2\pi/3a$ wave vector, and therefore its HOMO and LUMO are of the cosine type. The second tube does allow $k = 2\pi/3a$, and its solutions are of the sine type. The HOMO and LUMO correspond to the bonding and antibonding solutions, respectively (due to the shift of k_F towards *lower* values [3]; see below and Fig. 2). The experimentally observed effect of peak pairing [7] is explained by the asymmetric shapes of the lobes. A more direct comparison with the experimental 1D scans is shown in Fig. 1j where two possible scan lines are chosen on the tubes: (A) corresponds to the most common pattern with equidistant peaks separated by $\lambda_F/2 = 0.37$ nm, and (B) shows peak pairing within each λ_F, with distances of 0.25 and 0.50 nm in the chosen scan. The experimentally observed 0.32 and 0.43 nm distances [7] simply correspond to an intermediate scan line. In all cases the intermediate periods have to sum to the λ_F periodicity of the SW pattern (see Fig. 1). Furthermore, the results remain valid for other states above (below) the LUMO (HOMO) and if the diameter of the tube is increased to the experimental value of $\sim$1.3 nm [7].

The first-principles calculations were performed with tube lengths from 2 to 8 nm (up to 756 atoms) which show no differences even for the shortest tubes. The tube ends do not alter the observed images at the center of the tube and, therefore, do not affect the main conclusions of this Letter. However, they may give rise to states beyond the scope of the catalog of images presented above. In this Letter we have considered that the finite tube remains open after the local structural relaxation mentioned above. This particular ending produces one surface state at each end, 0.6 eV above the Fermi level that could play a role in field-emission process and chemical activity. Their shape is shown in Fig. 1g and can be accessible experimentally. The energy and shape of this state can be used as a fingerprint of the geometry of the tube end. Our general 3D catalog should be confirmed experimentally and extended to other chiralities.

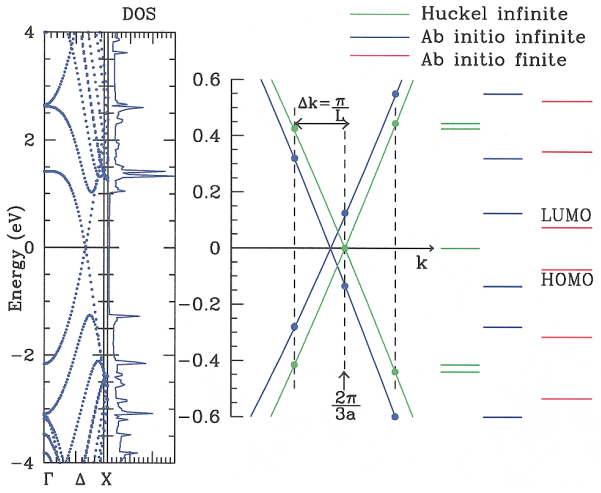

FIG. 2(color). Left: *ab initio* band structure and density of states (DOS) for an infinite (6, 6) carbon nanotube. The energy zero has been set at the Fermi level. Right: Magnification close to the Fermi level. Linear bands computed with the Hückel model (green) and the *ab initio* scheme (blue). Descending/ascending bands are of bonding/antibonding character in the bonds perpendicular to the tube axis. The vertical dashed lines indicate three allowed k values for a finite tube of length $L = 4.06$ nm. In a zone folding scheme, the energy levels of the finite tube are given by the band values at the allowed k points (shown as horizontal green and blue lines on the right, for the Hückel and *ab initio* calculations, respectively). Red lines show the levels obtained from the *ab initio* calculation on the finite and relaxed tube of the same length. The same relative behavior is obtained for longer tubes with a reduction of the average level spacing.

The gold surface can in principle affect the shape of the SW states. To study substrate effects we have performed first-principles calculations for a (5,5) nanotube on the Au(111) surface. A small charge transfer is observed from the gold substrate to the nanotube, mainly to the atoms closest to the substrate, which get charged by $\sim$0.1 extra electrons. Also, a strong binding of the tube to the surface is obtained (1.2 eV per tube unit cell). Both results agree with previous experimental observations [5,11] and indicate a preferential role of the substrate in the electronic structure of the nanotube. However, the shape of the wave functions at the tube resonances near the Fermi level show again a remarkable resemblance with those predicted in the catalog. Figure 1l shows one of them. We thus expect that the STS images of nanotubes on gold will still be those of the catalog predicted by the Hückel model, but we show below that this model is clearly insufficient to describe the energy dependence demonstrated by the experiments.

Both the Hückel model and the *ab initio* Hamiltonian of the infinite tube predict two sets of equidistant levels, one for each band, near the Fermi level. However, even at this level, the slightly different symmetry of the relaxed tube with respect to ideally wrapped graphene (as in Hückel) gives rise to a marked difference between both sets of levels, because the Fermi wave vector of the relaxed tube shifts towards values smaller than $2\pi/3a$ [2,3]. The absolute shift is enhanced by the difference in bond lengths after relaxation, and although the shift gets smaller with increasing diameter it is still important for sizes corresponding to the (10,10) nanotube. These differences and the asymmetries of the bands are evident in Fig. 2. The asymmetry right-left is responsible for the slight splitting of Hückel levels. The asymmetry up-down is absent in the Hückel model but evident in the *ab initio* band structure [3,9] and in experiments [4] and holds for all chiral and nonchiral single-wall nanotubes. A further important modification occurs (see Fig. 2) when the finite tubes are relaxed and their Hamiltonian is recalculated self-consistently (direct comparison with experiment is not provided since calculations for 30 nm tubes are out of reach). The value of the HOMO-LUMO gap decreases with increasing tube length not monotonically but exhibiting a well defined oscillation with a λ_F period that is related to the bonding character

of the HOMO and LUMO orbitals [12]. By increasing further the tube length we observe a smooth transition from an energy level structure characteristic of a molecular wire (zero-dimensional system) to that of a delocalized one-dimensional system that seems to be complete for tube lengths of the order or larger than 5 nm [12].

The gold substrate modifies the spectrum in several ways. It opens a small "pseudogap" in the tube states at the Fermi level whenever the symmetries of the tube are not respected by the substrate [21], as in this case. It breaks the validity of the two-band model due to the strong interaction between tube states and the empty Au(111)-surface state. It introduces some residual disorder that does not reduce the long electron mean free path [13] that does not destroy the standing-wave pattern of supported nanotubes. It also shifts the Fermi level, an effect related to the charge transfer mentioned above and seen in experiments [4]. Furthermore, the group velocity of the tube resonances near the Fermi level also changes. Therefore, although the SW images can be cataloged with a simple model, the energy spectrum requires the consideration of complex and subtle effects. It is remarkable that, even if the two-band model is no longer valid, the experimental energy levels close to the Fermi level seem to fit the simplest "1D particle-in-a-box model." However, the fact that states a few tenths of eV above or below the Fermi level are not resolved experimentally [7] supports our result of increasing hybridization between tube and gold states as we move away from the Fermi level. Similar results for STS image and energy levels will hold for nanotubes in ropes [22] opening a new technique to study the electronic structure of nanotubes (chiral and nonchiral ones). The complex low-energy features of supported carbon nanotubes are in need of further theoretical and experimental (transport and spectroscopic measurements) studies in order to assess the validity of the widely used "two-band model" and the role of correlations in this fascinating quasi-1D molecular-supported wires as main components in future molecular electronics and nanodevices [23].

We acknowledge financial support from DGES (Grant No. PB95-0202) and the computer facilities at C^4 (Centre de Computació i Comunicacions de Catalunya). We thank C. Dekker and L. C. Venema for sharing their experiments with us prior to publication and for useful discussions. We greatly benefited from discussions with S.G. Louie, Ph. Lambin, and J.C. Charlier.

*To whom correspondence should be addressed.
Email address: arubio@mileto.fam.cie.uva.es

[1] S. Iijima, Nature (London) **354**, 56 (1991).
[2] N. Hamada, S. Sawada, and A. Oshiyama, Phys. Rev. Lett. **68**, 1579 (1992).
[3] J. W. Mintmire, B. I. Dunlap, and C. T. White, Phys. Rev. Lett. **68**, 631 (1992).
[4] J. W. G. Wildöer, L. C. Venema, A. G. Rinzler, R. E. Smalley, and C. Dekker, Nature (London) **391**, 59 (1998); T. W. Odom, J.-L. Huang, P. Kim, and C. M. Lieber, Nature (London) **391**, 62 (1998).
[5] S. J. Tans, M. H. Devoret, H. Dai, A. Thess, R. E. Smalley, L. J. Geerligs, and C. Dekker, Nature (London) **386**, 474 (1997).
[6] M. Bockrath, D. H. Cobden, P. L. McEuen, N. G. Chopra, A. Zettl, A. Thess, and R. E. Smalley, Science **275**, 1922 (1997).
[7] L. C. Venema, J. W. G. Wildöer, S. J. Tans, J. W. Janssen, L. J. Hinne, T. Tuinstra, L. P. Kouwenhoven, and C. Dekker, Science **283**, 52 (1999).
[8] V. Meunier and Ph. Lambin, Phys. Rev. Lett. **81**, 5588 (1998).
[9] M. S. Dresselhaus, G. Dresselhaus, and P. C. Eklund, *Science of Fullerenes and Carbon Nanotubes* (Academic Press Inc., San Diego, 1996); T. W. Ebbesen, *Carbon nanotubes: preparation and properties* (CRC Press, New York, 1997).
[10] Ph. Lambin, A. Fonseca, J. P. Vigneron, J. B. Nagy, and R. E. Smalley, Chem. Phys. Lett. **245**, 87 (1995).
[11] L. C. Venema, J. W. C. Wildöer, T. Tuinstra, C. Dekker, A. G. Rinzler, and R. E. Smalley, Appl. Phys. Lett. **71**, 2629 (1997).
[12] H.-Y. Zhu, D. J. Klein, T. G. Schmalz, A. Rubio, and N. H. March, J. Phys. Chem. Solids **59**, 417 (1997); A. Rochefort, D. R. Salahub, and P. Avouris, e-print cond-mat/9808271.
[13] C. T. White and T. N. Todorov, Nature (London) **393**, 240 (1998). It is shown that conduction electrons in armchair nanotubes have very large electron mean free paths resulting in exceptional ballistic transport and localization lengths of 10 μm (long lifetime of the SW state).
[14] The Hamiltonian is $H_{ij} = -\gamma$ for neighbor atoms, and $H_{ij} = 0$ otherwise. It is known to provide an excellent description of the low-energy features for isolated armchair nanotubes [2,3], when $\gamma \sim -2.7$ eV.
[15] D. Sánchez-Portal, P. Ordejón, E. Artacho, and J. M. Soler, Int. J. Quantum Chem. **65**, 453 (1997); P. Ordejón, E. Artacho, and J. M. Soler, Phys. Rev. B **53**, R10 441 (1996).
[16] J. P. Perdew and A. Zunger, Phys. Rev. B **23**, 5048 (1981).
[17] N. Troullier and J. L. Martins, Phys. Rev. B **43**, 1993 (1991).
[18] O. F. Sankey and D. J. Niklewski, Phys. Rev. B **40**, 3979 (1989).
[19] J. Tersoff and D. Hamann, Phys. Rev. Lett. **50**, 1998 (1983).
[20] The experiments in Ref. [7] were performed in the constant-current mode. This means that each I-V curve has a different starting tube-tip height value for different points along the tube. This effect makes the quantitative comparison between theory and experiments more difficult but would not change the general shape of the electronic states in the catalog of Fig. 1.
[21] P. Delaney, H. J. Choi, J. Ihm, S. G. Louie, and M. L. Cohen, Nature (London) **391**, 466 (1998).
[22] W. Clauss, D. J. Bergeron, and A. T. Johnson, Phys. Rev. B **58**, R4266 (1998).
[23] P. G. Collins, A. Zettl, H. Bando, A. Thess, and R. E. Smalley, Science **278**, 100 (1997); S. J. Tans, A. R. M. Verschueren, and C. Dekker, Nature (London) **393**, 49 (1998).